AIMS Mathematics, 9(9): 25752–25775.
DOI: 10.3934/math.20241258
Received: 27 June 2024
Revised: 23 August 2024
Accepted: 30 August 2024
Published: 04 September 2024

https://www.aimspress.com/journal/Math

Research article

Adaptive state observer event-triggered consensus control for multi-agent systems with actuator failures

Kairui Chen[1], **Yongping Du**[1] **and Shuyan Xia**[1,2,*]

[1] School of Mechanical and Electrical Engineering, Guangzhou University, Guangzhou 510006, China

[2] School of Computer & Information, Qiannan Normal University for Nationalities, Duyun 558000, China

* **Correspondence:** Email: syxia@hnu.edu.cn; Tel: +15116263296.

Abstract: An adaptive neural network event-triggered consensus control method incorporating a state observer was proposed for a class of uncertain nonlinear multi-agent systems (MASs) with actuator failures. To begin, a state observer was constructed in an adaptive backstepping framework to estimate the MASs' unmeasurable states, and a radial basis function neural network (RBFNN) was employed to approximate the unknown nonlinear function of MASs. Meanwhile, to reduce the impact of actuator failure on the performance of MASs, the adaptive event-triggered mechanism (ETM) was designed to dynamically compensate for actuator failures, which alleviated the communication burden among individual agents by decreasing the update frequency of the control signals. Furthermore, all followers can track the leader's output signal with the synchronization errors converging to zero. Finally, simulation examples were used to verify the effectiveness of the proposed control strategy.

Keywords: multi-agent systems; consensus control; actuator failures; state observer design; event-triggered mechanism
Mathematics Subject Classification: 93A16, 93C10

1. Introduction

Currently, many engineering problems are complex and dynamic, posing challenges for traditional single-agent systems. Multi-agent systems (MASs) address these challenges through distributed problem-solving via collaboration, competition, and division of labor. Consequently, the coherent cooperative control of MASs has become a key research focus [1–7]. In [1], the authors studied the coherent adaptive cooperative control of uncertain nonlinear MASs from the three uncertainties of dead zone, disturbances, and uncertain time-varying control directions. Similarly, [3] extends the

investigation to include uncertainties such as unknown control directions, input unmodeled dynamics, sensor failures, and prescribed performance. In [5], a distributed control protocol is formulated through the integration of adaptive control techniques and matrix theory. The design incorporates Fourier series expansion and neural networks (NNs) to approximate uncertain nonlinearities with unmeasured periodic time-varying perturbations. A variety of industrial field agents are further reorganized into new heterogeneous MASs for cooperative control, and a review and outlook of the latest results are presented in [6]. However, all the above control methods presuppose the assumption that all states throughout the system can be measured.

The acquisition of state information is limited during the operational phase due to equipment constraints, various other variables, and environmental conditions [8–14]. These limitations hinder the system's tracking performance and stability. This constraint ultimately hinders the system's tracking performance and stability. In [8], heterogeneous MASs comprising numerous unmanned ground vehicles (UGVs) and unmanned aerial vehicles (UAVs) are investigated to design a fixed-time observer aimed at estimating the mismatch interference and set total uncertainty.

In [9], the aid of a fuzzy observer for estimating the unavailable states is accompanied by utilizing the characteristics of fuzzy logic systems (FLSs) to address mismatches among agents and uncertainties within the MASs. In [12], the combination of the designed NNs state observer with the introduced adaptive control algorithm addresses the system's steady-state control and transient performance. To deal with the problems arising from unknown perturbations, a low-coupling, simple structure and easy-to-implement nonlinear perturbation observer is designed in [14].

In addition, nonlinearities widely exist in engineering control systems, for instance, actuator failures are unavoidable problems that may negatively affect the stability, performance, safety, and lifetime of the system. Therefore, it is especially critical for systems that require a high degree of controllability and robustness. To cope with this problem, many scholars have proposed a multitude of innovative control schemes with adaptive backstepping control techniques as the research background [15–21]. In [15], an adaptive fuzzy fixed-time fault-tolerant controller was designed by utilizing the inverse step control technique and the fixed-time stabilization theory. In [16], an adaptive output feedback compensation method is proposed by considering both actuator and sensor failure. Compared with [16] Authors in [17] relaxes the assumption requirement on the nonlinear functions, and proposes a new compensation mechanism to compensate for the impact of actuator failures by employing the approach of cubic absolute value Lyapunov functions and the novel (σ, σ^f)-modification.

On the contrary, the aforementioned research accomplishments rely on a traditional time-triggered mechanism (TTM). The fixed sample frequency and limitations in communication bandwidth associated with TTM lead to data redundancy in network signal transmission, thus occupying communication resources. Consequently, there has been a growing interest among scholars in exploring the event-triggered mechanism (ETM) [22–30]. In [22], an event-triggered output feedback control method incorporating adaptive dynamic programming (ADP) with a state observer is proposed to reduce the signal transmissions on network channels, and thus control signals are updated only at specific moments where the triggering conditions are violated. In [25], researchers construct an adaptive progressive tracking control strategy with a temporal control mechanism and an event triggering mechanism with variable thresholds, and comparative experiments indicate better robustness with the latter. In [27], the combination of command filtering backstepping and adaptive event-triggered communication (e.g., when a certain threshold is reached) solves the virtual controller

complexity problem while effectively avoiding the waste of communication resources. While [29] is opposite to [27, 29], the preset triggered condition is established by utilizing the negative semi-definiteness of the Lyapunov function's derivative, aiming to alleviate the communication burden and conserve computational resources.

In summary, with regard to a category of uncertain nonlinear MASs with actuator failures, an adaptive NNs event-triggered consensus control strategy incorporating the state observer is proposed to reduce the impact of the system by actuator failures. In comparison to existing findings, the main innovations of the proposed control method include:

(1) Different from the existing algorithms, such as [15, 16, 27] an event-triggered adaptive states observation consistency control strategy is proposed for a class of uncertain nonlinear MASs with actuator failures.
(2) With regard to the actuator failures that are common in the actual industrial production system, the existing compensation programs, such as [17–20], need to occupy a large amount of communication resources. Thus, the design of an adaptive ETM to achieve dynamic compensation for actuator failures while reducing the update frequency of control signals, which reduces the occupation of communication resources, is more widespread in practical engineering.
(3) Due to the actual systems, the states of the system are often unmeasurable and the system is characterized by nonlinearities. Therefore, an adaptive NNs control method incorporating a state observer is proposed, which utilizes radial basis function neural networks (RBFNNs) to approximate MASs' unknown nonlinear functions, and the state observer is formulated for estimating the states of MASs.

The rest is presented in the following sections. Section 2 contains the problem description and preliminaries. Section 3 designs an adaptive NNs event-triggered consensus control scheme. Section 4 gives two simulation examples to verify the effectiveness of the designed scheme. Section 5 is the conclusion.

2. Problem description and preliminaries

2.1. Problem description

Consider the following category of uncertain nonlinear MASs [31]

$$\begin{cases} \dot{x}_{k,i} = x_{k,i+1} + f_{k,i}(X_{k,i}), i = 1, 2, \ldots, n-1 \\ \dot{x}_{k,n} = u_k + f_{k,n}(X_{k,n}) \\ y_k = x_{k,1} \end{cases} \tag{2.1}$$

where $X_{k,i} = [x_{k,1}, x_{k,2}, \ldots, x_{k,i}]^T$ and $X_{k,n} = [x_{k,1}, x_{k,2}, \ldots, x_{k,n}]^T$ are the state vectors, which are not measurable; $f_{k,i}(\cdot)$ is the unknown smooth nonlinear function; u_k represents the control input, while $y_k \in [y_{k,1}, y_{k,2}, \ldots, y_{k,n}]^T$ denotes system output. The system consists of a leader labeled G and $k(k = 1, 2, \ldots, N)$ followers.

Assume each agent is equipped with $b = 1, 2, \ldots, Z, (Z > 1)$ actuators, where $u_k = \sum_{b=1}^{Z} l_{k,b} u_{k,b}$ and $l_{k,b}$ denotes the known constant control gain. During actual operation, agents will inevitably suffer

from actuator failures. The actuator failure model of $b-th$ $(1,2,\ldots,Z)$ is given as follows:

$$\begin{cases} u_{k,b} = \rho_{k,b}\bar{u}_{k,b} + c_{k,b}, \forall t \geq t_{bw} \\ \rho_{k,b}c_{k,b} = 0 \end{cases} \tag{2.2}$$

where the health factor is $\rho_{k,b} \in [0,1]$; $c_{k,b}$ and t_{bw} are unknown constants, t_{bw} indicates the moment of the bth actual failure. The crucial working states of the actuator operation are categorized into three situations:

1) $\rho_{k,b} = 0$, $u_{k,b} = c_{k,b}$. The actuator is in a state of complete failure.

2) $\rho_{k,b} \in (0,1)$, $u_{k,b} = \rho_{k,b}\bar{u}_{k,b}$. The partial failure will occur during actuator working.

3) $\rho_{k,b} = 1$, $u_{k,b} = \bar{u}_{k,b}$. The actuator works properly.

To facilitate the subsequent analysis, the work situations of the three actuators mentioned above are further summarized. Thus, two sets L_{m1} and L_{m2} are set and $L_{m1} \cup L_{m2} = \{1,2,\ldots,Z\}$. Here, L_{m1} indicates that the actuator is in a set of partial failure and normal operating states; L_{m2} denotes the set in which the actuator is in a complete failure state.

Then, the MASs (2.1) is transformed into the following equation:

$$\begin{cases} \dot{X}_k = A_e X_k + Hy_k + \sum_{i=1}^{n} R_{k,i} f_{k,i}(X_{k,i}) + R_{k,n}u_k \\ y_k = Q^T X_k \end{cases} \tag{2.3}$$

where

$$A_e = \begin{bmatrix} -h_{k,1} & 1 & \cdots & 0 \\ \vdots & \vdots & \ddots & \vdots \\ -h_{k,n-1} & 0 & \cdots & 1 \\ -h_{k,n} & 0 & \cdots & 0 \end{bmatrix}_{n\times n} \quad H = \begin{bmatrix} h_{k,1} \\ \vdots \\ h_{k,n-1} \\ h_{k,n} \end{bmatrix} R_{k,i} = \left[\underbrace{0\cdots 1}_{i}\cdots 0\right]^T \quad R_{k,n} = \left[\underbrace{0\cdots 1}_{n}\right]^T \quad Q = [1,0,\cdots,0]^T$$

where A_e is a strict Hurwitz matrix. Given a positive definite matrix $P = P^T > 0$, there exists a positive definite matrix $O = O^T > 0$, which satisfies $A_e^T O + OA_e = -P$.

Assumption 1 ([32]). *The desired trajectory $y_s = [y_{s1}, y_{s2}, \ldots, y_{sn}]^T \in R^n$ has the derivative of the $(n+1)-th$ order. There are constants $s_0 > 0$ and $s_1 > 0$ such that $s_1 > s_0$ and $|y_s| \leq s_0 \leq s_1$.*

Assumption 2 ([33]). *During the operation, the system can stand $Z-1$ actuator failures at the same time to the greatest extent.*

Lemma 1 ([34]). *For any $\upsilon, \varrho \in \mathcal{R}$, the following inequality holds for*

$$0 \leq |\upsilon| - \upsilon \tanh\left(\frac{\upsilon}{\varrho}\right) \leq 0.2785\varrho. \tag{2.4}$$

2.2. Graph theory

Through a directed graph $\mathcal{Q}(\mathcal{F}, \mathfrak{D})$, the communication topology among agents including leaders and followers is presented, in which $\mathcal{F} = \{G, 1, 2, \ldots, N\}$ represents the set of agents and $\mathfrak{D} \subseteq \mathcal{F} \times \mathcal{F}$ denotes the set of edges. $\mathbf{A} = [a_{kj}]_{N\times N}$ signifies the adjacency matrix of the graph $\mathcal{Q}$ between agents. If there is an edge $(j,k) \subseteq \mathfrak{D}$ (from agent j to agent k), which signifies that agent k can receive information from agent j, then $a_{kj} > 0$; contrarily, $a_{kj} = 0$. In addition, a matrix $\mathbf{D} = diag\{s_1, s_2, .., s_N\} \in R^{N\times N}$ is obtained, in which $s_i = \sum_{j=1}^{N} a_{kj}$, $i = 1,2,\ldots,N$, and a Laplacian matrix is $\mathbf{L} = \mathbf{D} - \mathbf{A} \in R^{N\times N}$.

2.3. RBFNNs

By using the characteristic that NNs can arbitrarily approximate the unknown nonlinear function, the unknown nonlinear function of $Q(\theta)$ is processed, and there are

$$Q(\theta) = \psi^T W(\theta) + \varepsilon(\theta) \tag{2.5}$$

where $W(\theta) = [W_1(\theta), W_2(\theta), \ldots, W_n(\theta)]^T$ is expressed as the basis function vector and $\psi = [\psi_1, \psi_2, \ldots, \psi_n]^T$ signifies the ideal weight vector, in which $n > 0$ is the number of neural nodes; there exists a positive constant $\bar{\varepsilon}$ denoted as the approximation error such that $|\varepsilon(\theta)| \leq \bar{\varepsilon}$. Generally, the following basis function is selected as

$$W_i(\theta) = -\exp\left(\frac{(\theta - p_i)^T(\theta - p_i)}{\kappa_i^2}\right) \tag{2.6}$$

where $i = 1, 2, \ldots, n$; κ_i signifies the width, while $p_i = [p_{i1}, p_{i2}, \ldots, p_{in}]^T$ denotes the center of the Gaussian function.

Remark 1. *$\psi \in R^{\iota}$ encompasses ι unknown constants, represented by an unknown constant value ζ for $\|\psi\|^2 = \zeta$. By updating the norm of ψ instead of directly estimating it, thus, only the parameter ζ is estimated. This is done to minimize the estimation error $\tilde{\zeta} = \zeta - \hat{\zeta}$, thereby reducing computational load and simplifying controller design.*

3. Adaptive NNs event-triggered consensus control design

3.1. State observer design

Since the states of the MASs are unmeasurable, the following state observer is designed for its estimation and its expression is

$$\begin{cases} \dot{\hat{x}}_{k,i} = \hat{x}_{k,n} + h_i(y_k - \hat{x}_{k,1}) \\ \dot{\hat{x}}_{k,n} = \sum_{b=1}^{Z} l_{k,b}u_{k,b} + h_n(y_k - \hat{x}_{k,1}) \end{cases} \tag{3.1}$$

where $\hat{X}_{k,i} = [\hat{x}_{k,1}, \hat{x}_{k,2}, \cdots, \hat{x}_{k,i}]^T$ is the estimated value of $X_{k,i}$ and $\hat{X}_{k,n} = [\hat{x}_{k,1}, \hat{x}_{k,2}, \cdots, \hat{x}_{k,n}]^T$ is the estimated value of $X_{k,n}$. The observer error is $e_k = X_{k,n} - \hat{X}_{k,n}$, and its derivative is obtained as

$$\dot{e}_k = Ae_k + \sum_{q=1}^{n} B_{k,q}f_{k,q}. \tag{3.2}$$

Select the following Lyapunov function:

$$V_{k,0} = e_k^T O_k e_k. \tag{3.3}$$

By taking the derivative of $V_{k,0}$, one has

$$\dot{V}_{k,0} = e_k^T(A_e^T O_k + O_k A_e)e_k + e_k^T O_k \left(\sum_{q=1}^{n} B_{k,q} f_{k,q} \right)$$
$$= -e_k^T P_k e_k + 2e_k^T O_k \left(\sum_{q=1}^{n} B_{k,q} f_{k,q} \right). \tag{3.4}$$

According to Young's inequality and $\sum_{i=1}^{n} W_{k,0}^T W_{k,0} \leq 1$. Additionally, ζ is defined as $\zeta = max\left\{n\|\psi_0\|^2, \|\psi_i\|^2, i = 1, \ldots, n\right\}$ and n is the number of neural nodes. Therefore, there will be $\|\psi_0\|^2 \leq \zeta/n$, and $\left|\varepsilon_{k,0}\right| \leq \bar{\varepsilon}_{k,0}$ represents the approximate error, $\bar{\varepsilon}_{k,0} > 0$.

$$2e_k^T O_k \sum_{q=1}^{n} B_{k,q} f_{k,q} = 2e_k^T O_k \sum_{q=1}^{n} B_{k,q} \left(\tilde{\psi}_{k,0}^T W_{k,0} + \varepsilon_{k,0} \right)$$
$$\leq 2\lambda_{max}^2(O_k)\|e_k\|^2 + \|O_k\|^2 \zeta_k + \|O_k\|^2 \bar{\varepsilon}_{k,0}^2. \tag{3.5}$$

Then, substitute (3.5) into (3.4) to get

$$\dot{V}_{k,0} \leq -\Delta\|e_k\|^2 + \|O_k\|^2 \left(\zeta_k + \bar{\varepsilon}_{k,0}^2 \right) \tag{3.6}$$

where $\Delta = -2\left(\lambda_{max}(O_k)\right)^2 + \lambda_{min}(P_k)$.

3.2. Control design

The construction of virtual control laws within the backstepping control framework follows. Initially, the error system is expressed as

$$\begin{cases} z_{k,1} = \upsilon_k(y_k - y_s) + \sum_{j=1}^{N} a_{kj}(y_k - y_j) \\ z_{k,n} = \hat{x}_{k,n} - \alpha_{k,n-1} \quad (n \geq 2) \end{cases} \tag{3.7}$$

where $z_{k,1}$ and $z_{k,n}$ represent a synchronization error of agent k and a virtual error, respectively; y_s is the leader's output signal; $\upsilon_k \geq 0$ denotes the weight vector associated with the edge from agent k to leader G. In particular, when $\upsilon_k = 0$, it means that there is no direct information exchange between agent k and leader G. Moreover, at least one agent will receive the synchronization information from leader G.

Step 1: The first Lyapunov function is constructed as follows:

$$V_{k,1} = V_{k,0} + \frac{1}{2} z_{k,1}^2 + \frac{1}{2r_{k,1}} \tilde{\zeta}_{k,1}^2 \tag{3.8}$$

where $r_{k,1} > 0$ is a constant. $\tilde{\zeta}_{k,1} = \zeta_{k,1} - \hat{\zeta}_{k,1}$ signifies the estimation error, and $\hat{\zeta}_{k,1}$ represents the estimation of the uncertain parameter $\zeta_{k,1}$. Then, from (2.1) and (3.7), the derivation of $z_{k,1}$ is

$$\dot{z}_{k,1} = (\upsilon_k + s_k)(e_{k,2} + z_{k,2} + \alpha_{k,1} + f_{k,1}) - \dot{y}_s \upsilon_k - \sum_{j=1}^{N} a_{kj}(x_{j,2} + f_{j,1}). \tag{3.9}$$

According to (3.9), the $\dot{V}_{k,1}$ has

$$\dot{V}_{k,1} = \dot{V}_{k,0} + z_{k,1}(\upsilon_k + s_k)(e_{k,2} + z_{k,2} + \alpha_{k,1} + f_{k,1}) - \dot{y}_s\upsilon_k - \sum_{j=1}^{N} a_{kj}(x_{j,2} + f_{j,1}) - \frac{1}{r_{k,1}}\tilde{\zeta}_{k,1}\dot{\hat{\zeta}}_{k,1}. \tag{3.10}$$

Utilizing Young's inequality yields

$$z_{k,1}(\upsilon_k + s_k)e_{k,2} \leq \frac{1}{4}z_{k,1}^2(\upsilon_k + s_k)^2 + \|e_k\|^2. \tag{3.11}$$

Let $Q_{k,1}(\theta_{k,1}) = (\upsilon_k + s_k)f_{k,1} + \frac{1}{4}z_{k,1}(\upsilon_k + s_k)^2 - \dot{y}_s\upsilon_k - \sum_{j=1}^{N} a_{kj}(x_{j,2} + f_{j,1})$, the unknown nonlinear function $Q_{k,1}(\theta_{k,1})$ is approximated by RBFNN, and it obtained that

$$Q_{k,1}(\theta_{k,1}) = \psi_{k,1}^T W_{k,1}(\theta_{k,1}) + \varepsilon_{k,1}(\theta_{k,1}) \tag{3.12}$$

where $\theta_{k,1} = [\hat{x}_{k,1}, \hat{x}_{j,1}, \hat{x}_{j,2}, \dot{y}_s]^T$. Utilizing Young's inequality yields

$$\begin{aligned} z_{k,1}Q_{k,1}(\theta_{k,1}) =& z_{k,1}\psi_{k,1}^T W_{k,1}(\theta_{k,1}) + z_{k,1}\varepsilon_{k,1}(\theta_{k,1}) \\ \leq& \frac{1}{2\sigma_{k,1}^2}z_{k,1}^2\zeta_{k,1}\left\|W_{k,1}\right\|^2 + \frac{\sigma_{k,1}^2}{2} + \frac{z_{k,1}^2}{2} + \frac{\bar{\varepsilon}_{k,1}^2}{2} \end{aligned} \tag{3.13}$$

where $\zeta_{k,1} = \left\|\psi_{k,1}\right\|^2$, $\sigma_{k,1}$ is a positive constant to be designed, and $\left|\varepsilon_{k,1}\right| \leq \bar{\varepsilon}_{k,1}$ represents the approximate error, $\bar{\varepsilon}_{k,1} > 0$.

By incorporating (3.11)–(3.13) into (3.10) yields

$$\begin{aligned} \dot{V}_{k,1} \leq& \dot{V}_{k,0} + z_{k,1}\left((\upsilon_k + s_k)\alpha_{k,1} + \frac{1}{2\sigma_{k,1}^2}z_{k,1}\hat{\zeta}_{k,1}\left\|W_{k,1}\right\|^2\right) + \frac{z_{k,1}^2}{2} + \frac{\sigma_{k,1}^2}{2} + \frac{\bar{\varepsilon}_{k,1}^2}{2} \\ &- \frac{1}{r_{k,1}}\tilde{\zeta}_{k,1}\left(\dot{\hat{\zeta}}_{k,1} - \frac{1}{2\sigma_{k,1}^2}r_{k,1}z_{k,1}^2\left\|W_{k,1}\right\|^2\right) + (\upsilon_k + s_k)z_{k,1}z_{k,2}. \end{aligned} \tag{3.14}$$

$\alpha_{k,1}$ and $\dot{\hat{\zeta}}_{k,1}$ are designed as

$$\alpha_{k,1} = -\frac{1}{(\upsilon_k + s_k)}\left(\beta_{k,1}z_{k,1} + \frac{1}{2\sigma_{k,1}^2}z_{k,1}\hat{\zeta}_{k,1}\left\|W_{k,1}\right\|^2\right), \tag{3.15}$$

$$\dot{\hat{\zeta}}_{k,1} = \frac{1}{2\sigma_{k,1}^2}r_{k,1}z_{k,1}^2\left\|W_{k,1}\right\|^2 - \xi_{k,1}\hat{\zeta}_{k,1}, \tag{3.16}$$

where $\beta_{k,1} > 0$ and $\xi_{k,1} > 0$ are constants.

By incorporating (3.15)-(3.16) into (3.14) yields

$$\dot{V}_{k,1} \leq -\Delta_1\|e_k\|^2 + M_1 - \beta_{k,1}z_{k,1}^2 + \frac{1}{r_{k,1}}\xi_{k,1}\tilde{\zeta}_{k,1}\hat{\zeta}_{k,1} + (\upsilon_k + s_k)z_{k,1}z_{k,2} + \frac{\sigma_{k,1}^2}{2} + \frac{\bar{\varepsilon}_{k,1}^2}{2} + \frac{z_{k,1}^2}{2} \tag{3.17}$$

where $\Delta_1 = \Delta - 1$ and $M_1 = \|O_k\|^2\left(\zeta_k + \bar{\varepsilon}_{k,0}^2\right)$.

Step i ($i = 2, 3, \ldots, n-1$): The Lyapunov function is constructed as

$$V_{k,i} = V_{k,i-1} + \frac{1}{2}z_{k,i}^2 + \frac{1}{2r_{k,i}}\tilde{\zeta}_{k,i}^2, \tag{3.18}$$

where $\tilde{\zeta}_{k,i} = \zeta_{k,i} - \hat{\zeta}_{k,i}$ signifies the estimation error, and $\hat{\zeta}_{k,i}$ represents the estimation of the uncertain parameter $\zeta_{k,i}$. According to (3.7), one has

$$\dot{z}_{k,i} = z_{k,i+1} + \alpha_{k,i} + h_i(y_k - \hat{x}_{k,1}) - \dot{\alpha}_{k,i-1} \tag{3.19}$$

where

$$\begin{aligned}\dot{\alpha}_{k,i-1} =& \sum_{q=1}^{i-1}\frac{\partial\alpha_{k,i-1}}{\partial\hat{x}_{k,q}}(\hat{x}_{k,q+1} + h_q e_{k,1}) + \sum_{q=1}^{i-1}\frac{\partial\alpha_{k,i-1}}{\partial\hat{\zeta}_{k,q}}\dot{\hat{\zeta}}_{k,q} + \frac{\partial\alpha_{k,i-1}}{\partial x_{k,1}}(e_{k,2} + \hat{x}_{k,2} + f_{k,1}) \\ &+ \sum_{q=1}^{i-1}\sum_{j=1}^{N}\frac{\partial\alpha_{k,i-1}}{\partial\hat{x}_{j,q}}\dot{x}_{j,q} + \sum_{q=1}^{i}\frac{\partial\alpha_{k,i-1}}{\partial y_s^{(q-1)}}\dot{y}_s^{(q)}.\end{aligned} \tag{3.20}$$

According to (3.19)-(3.20), one has

$$\begin{aligned}\dot{V}_{k,i} =& \dot{V}_{k,i-1} + z_{k,i}\Bigg(z_{k,i+1} + \alpha_{k,i} + h_i(y_k - \hat{x}_{k,1}) - \sum_{q=1}^{i-1}\frac{\partial\alpha_{k,i-1}}{\partial\hat{x}_{k,q}}(\hat{x}_{k,q+1} + h_q e_{k,1}) - \sum_{q=1}^{i-1}\frac{\partial\alpha_{k,i-1}}{\partial\hat{\zeta}_{k,q}}\dot{\hat{\zeta}}_{k,q} \\ &- \frac{\partial\alpha_{k,i-1}}{\partial x_{k,1}}(e_{k,2} + \hat{x}_{k,2} + f_{k,1}) - \sum_{q=1}^{i-1}\sum_{j=1}^{N}\frac{\partial\alpha_{k,i-1}}{\partial\hat{x}_{j,q}}\dot{x}_{j,q} - \sum_{q=1}^{i}\frac{\partial\alpha_{k,i-1}}{\partial y_s^{(q-1)}}\dot{y}_s^{(q)}\Bigg) - \frac{1}{r_{k,1}}\tilde{\zeta}_{k,i}\dot{\hat{\zeta}}_{k,i}.\end{aligned} \tag{3.21}$$

Utilizing the Young's inequality yields

$$-z_{k,i}\frac{\partial\alpha_{k,i-1}}{\partial_{k,i}}e_{k,2} \le \frac{1}{4}z_{k,i}^2\left(\frac{\partial\alpha_{k,i-1}}{\partial_{k,i}}\right)^2 + \|e_k\|^2. \tag{3.22}$$

If $i = 2$, let $Q_{k,i}(\theta_{k,i}) = h_i(y_k - \hat{x}_{k,1}) - \sum_{q=1}^{i-1}\frac{\partial\alpha_{k,i-1}}{\partial\hat{x}_{k,q}}(\hat{x}_{k,q+1} + h_q e_{k,1}) - \sum_{q=1}^{i-1}\frac{\partial\alpha_{k,i-1}}{\partial\hat{\zeta}_{k,q}}\dot{\hat{\zeta}}_{k,q} - \frac{\partial\alpha_{k,i-1}}{\partial x_{k,1}}(\hat{x}_{k,2} + f_{k,1}) - \sum_{q=1}^{i-1}\sum_{j=1}^{N}\frac{\partial\alpha_{k,i-1}}{\partial\hat{x}_{j,q}}\dot{x}_{j,q} - \sum_{q=1}^{i}\frac{\partial\alpha_{k,i-1}}{\partial y_s^{(q-1)}}\dot{y}_s^{(q)} + \frac{1}{4}z_{k,i}^2\left(\frac{\partial\alpha_{k,i-1}}{\partial_{k,i}}\right)^2 + \frac{z_{k,i-1}^2}{2} + (\upsilon_k + s_k)z_{k,i-1}$. If $i \ge 3$, let $Q_{k,i}(\theta_{k,i}) = h_i(y_k - \hat{x}_{k,1}) - \sum_{q=1}^{i-1}\frac{\partial\alpha_{k,i-1}}{\partial\hat{x}_{k,q}}(\hat{x}_{k,q+1} + h_q e_{k,1}) - \sum_{q=1}^{i-1}\frac{\partial\alpha_{k,i-1}}{\partial\hat{\zeta}_{k,q}}\dot{\hat{\zeta}}_{k,q} - \frac{\partial\alpha_{k,i-1}}{\partial x_{k,1}}(\hat{x}_{k,2} + f_{k,1}) - \sum_{q=1}^{i-1}\sum_{j=1}^{N}\frac{\partial\alpha_{k,i-1}}{\partial\hat{x}_{j,q}}\dot{x}_{j,q} - \sum_{q=1}^{i}\frac{\partial\alpha_{k,i-1}}{\partial y_s^{(q-1)}}\dot{y}_s^{(q)} + \frac{1}{4}z_{k,i}^2\left(\frac{\partial\alpha_{k,i-1}}{\partial_{k,i}}\right)^2 + \frac{z_{k,i-1}^2}{2} + z_{k,i-1}$. Then, the unknown nonlinear function $Q_{k,i}(\theta_{k,i})$ is approximated by an RBFNN, and it is obtained that

$$Q_{k,i}(\theta_{k,i}) = \psi_{k,i}^T W_{k,i}(\theta_{k,i}) + \varepsilon_{k,i}(\theta_{k,i}) \tag{3.23}$$

where $\theta_{k,i} = [\hat{x}_{k,i}^T, \hat{x}_{j,i}^T, \dot{y}_s]^T$. Applying Young's inequality yields

$$\begin{aligned}z_{k,i}Q_{k,i}(\theta_{k,i}) =& z_{k,i}\psi_{k,i}^T W_{k,i}(\theta_{k,i}) + z_{k,i}\varepsilon_{k,i}(\theta_{k,i}) \\ \le& \frac{1}{2\sigma_{k,i}^2}z_{k,i}^2\zeta_{k,i}\left\|W_{k,i}\right\|^2 + \frac{\sigma_{k,i}^2}{2} + \frac{z_{k,i}^2}{2} + \frac{\bar{\varepsilon}_{k,i}^2}{2}\end{aligned} \tag{3.24}$$

where $\zeta_{k,i} = \left\|\psi_{k,i}\right\|^2$, $\sigma_{k,i}$ is a positive constant to be designed, and $\left|\varepsilon_{k,i}\right| \leq \bar{\varepsilon}_{k,i}$ represents the approximate error, $\bar{\varepsilon}_{k,i} > 0$.

By incorporating (3.22)–(3.24) into (3.21) yields

$$\begin{aligned}\dot{V}_{k,i} \leq & -\Delta_i \left\|e_k\right\|^2 + M_1 + z_{k,1}\left(\alpha_{k,i} + \frac{1}{2\sigma_{k,i}^2} z_{k,1}\hat{\zeta}_{k,i}\left\|W_{k,i}\right\|^2\right) + \frac{z_{k,i}^2}{2} + z_{k,i}z_{k,i+1} \\ & - \frac{1}{r_{k,i}}\tilde{\zeta}_{k,i}\left(\dot{\hat{\zeta}}_{k,i} - \frac{1}{2\sigma_{k,i}^2} r_{k,i}z_{k,i}^2\left\|W_{k,i}\right\|^2\right) + \sum_{q=1}^{i}\left(\frac{\sigma_{k,q}^2}{2} + \frac{\bar{\varepsilon}_{k,q}^2}{2}\right).\end{aligned} \tag{3.25}$$

$\alpha_{k,i}$ and $\dot{\hat{\zeta}}_{k,i}$ are designed as

$$\alpha_{k,i} = -\beta_{k,i}z_{k,i} - \frac{1}{2\sigma_{k,i}^2} z_{k,i}\hat{\zeta}_{k,i}\left\|W_{k,i}\right\|^2, \tag{3.26}$$

$$\dot{\hat{\zeta}}_{k,i} = \frac{1}{2\sigma_{k,i}^2} r_{k,i}z_{k,i}^2\left\|W_{k,i}\right\|^2 - \xi_{k,i}\hat{\zeta}_{k,i}, \tag{3.27}$$

where $\beta_{k,i}$ and $\xi_{k,i}$ are positive constants to be designed.

Further, by incorporating (3.26)-(3.27) into (3.25) yields

$$\dot{V}_{k,i} \leq -\Delta_i \left\|e_k\right\|^2 + M_1 - \beta_{k,i}z_{k,i}^2 + \frac{z_{k,i}^2}{2} + z_{k,i}z_{k,i+1} + \frac{1}{r_{k,i}}\xi_{k,i}\tilde{\zeta}_{k,i}\hat{\zeta}_{k,i} + \sum_{q=1}^{i}\left(\frac{\sigma_{k,q}^2}{2} + \frac{\bar{\varepsilon}_{k,q}^2}{2}\right). \tag{3.28}$$

Step n: Construct the Lyapunov function as

$$V_{k,n} = V_{k,n-1} + \frac{1}{2}z_{k,n}^2 + \frac{1}{2r_{k,n}}\tilde{\zeta}_{k,n}^2 + \sum_{b=1,b\in L_{m1}}^{Z}\frac{1}{2}\left|l_{k,b}\right|\rho_{k,b}\tilde{K}_{k,b}^T\Gamma_{k,b}^{-1}\tilde{K}_{k,b} \tag{3.29}$$

where $r_{k,n}$ is a positive constant to be designed. $\tilde{\zeta}_{k,n} = \zeta_{k,n} - \hat{\zeta}_{k,n}$ signifies the estimation error, and $\hat{\zeta}_{k,n}$ represents the estimation of the uncertain parameter $\zeta_{k,n}$. $\Gamma_{k,b}^{-1}$ is the inverse matrix of $\Gamma_{k,b}$, which moreover denotes a positive definite matrix.

Since the $\dot{z}_{k,n} = \sum_{b=1}^{Z} l_{k,b}\left(\bar{u}_{k,b}\rho_{k,b} + c_{k,b}\right) + h_n(y_k - \hat{x}_{k,1}) - \dot{\alpha}_{k,n-1}$, it is the same as ***Step i***.

$$\begin{aligned}\dot{\alpha}_{k,n-1} = & \sum_{q=1}^{n-1}\frac{\partial\alpha_{k,n-1}}{\partial\hat{x}_{k,q}}(\hat{x}_{k,q+1} + h_q e_{k,1}) + \sum_{q=1}^{n-1}\frac{\partial\alpha_{k,n-1}}{\partial\hat{\zeta}_{k,q}}\dot{\hat{\zeta}}_{k,q} + \frac{\partial\alpha_{k,n-1}}{\partial x_{k,1}}(e_{k,2} + \hat{x}_{k,2} + f_{k,1}) \\ & + \sum_{q=1}^{n-1}\sum_{j=1}^{N}\frac{\partial\alpha_{k,n-1}}{\partial\hat{x}_{j,q}}\dot{x}_{j,q} + \sum_{q=1}^{n}\frac{\partial\alpha_{k,n-1}}{\partial y_s^{(q-1)}}\dot{y}_s^{(q)}.\end{aligned} \tag{3.30}$$

The expression for $V_{k,n}$ after derivation is

$$\begin{aligned}\dot{V}_{k,n} =&\dot{V}_{k,n-1} + z_{k,n}\left(\sum_{b=1}^{Z} l_{k,b}\left(\bar{u}_{k,b}\rho_{k,b} + c_{k,b}\right) + h_n(y_k - \hat{x}_{k,1}) - \sum_{q=1}^{n-1}\frac{\partial\alpha_{k,n-1}}{\partial\hat{x}_{k,q}}(\hat{x}_{k,q+1} + h_q e_{k,1})\right.\\ &- \sum_{q=1}^{n-1}\frac{\partial\alpha_{k,n-1}}{\partial\hat{\zeta}_{k,q}}\dot{\hat{\zeta}}_{k,q} - \frac{\partial\alpha_{k,n-1}}{\partial x_{k,1}}(e_{k,2} + \hat{x}_{k,2} + f_{k,1}) - \sum_{q=1}^{n-1}\sum_{j=1}^{N}\frac{\partial\alpha_{k,n-1}}{\partial\hat{x}_{j,q}}\dot{x}_{j,q} - \left.\sum_{q=1}^{n}\frac{\partial\alpha_{k,n-1}}{\partial y_s^{(q-1)}}\dot{y}_s^{(q)}\right)\\ &- \frac{1}{r_{k,1}}\tilde{\zeta}_{k,n}\dot{\hat{\zeta}}_{k,n} - \sum_{b=1}^{Z}|l_{k,b}|\rho_{k,b}\tilde{K}_{k,b}^{-1}\Gamma_{k,b}^{-1}\dot{\hat{K}}_{k,b}.\end{aligned} \tag{3.31}$$

Utilizing Young's inequality yields

$$-z_{k,n}\frac{\partial\alpha_{k,n-1}}{\partial_{k,n}}e_{k,2} \le \frac{1}{4}z_{k,n}^2\left(\frac{\partial\alpha_{k,n-1}}{\partial_{k,n}}\right)^2 + \|e_k\|^2. \tag{3.32}$$

Let $Q_{k,n}(\theta_{k,n}) = h_n(y_k - \hat{x}_{k,1}) - \sum_{q=1}^{n-1}\frac{\partial\alpha_{k,n-1}}{\partial\hat{x}_{k,q}}(\hat{x}_{k,q+1} + h_q e_{k,1}) - \sum_{q=1}^{n-1}\frac{\partial\alpha_{k,n-1}}{\partial\hat{\zeta}_{k,q}}\dot{\hat{\zeta}}_{k,q} - \frac{\partial\alpha_{k,n-1}}{\partial x_{k,1}}(\hat{x}_{k,2} + f_{k,1}) - \sum_{q=1}^{n-1}\sum_{j=1}^{N}\frac{\partial\alpha_{k,n-1}}{\partial\hat{x}_{j,q}}\dot{x}_{j,q} - \sum_{q=1}^{n}\frac{\partial\alpha_{k,n-1}}{\partial y_s^{(q-1)}}\dot{y}_s^{(q)} + \frac{1}{4}z_{k,n}^2\left(\frac{\partial\alpha_{k,n-1}}{\partial_{k,n}}\right)^2 + \frac{z_{k,n-1}^2}{2} + z_{k,n-1}$. Then, the unknown nonlinear function $Q_{k,n}(\theta_{k,n})$ is approximated by an RBFNN, and it is obtained that

$$Q_{k,n}(\theta_{k,n}) = \psi_{k,n}^T W_{k,n}(\theta_{k,n}) + \varepsilon_{k,n}(\theta_{k,n}) \tag{3.33}$$

where $\theta_{k,n} = [\hat{x}_{k,n}^T, \hat{x}_{j,n}^T, \dot{y}_s]^T$. Applying Young's inequality, one has

$$\begin{aligned}z_{k,n}Q_{k,n}(\theta_{k,n}) =&z_{k,n}\psi_{k,n}^T W_{k,n}(\theta_{k,n}) + z_{k,n}\varepsilon_{k,n}(\theta_{k,n})\\ \le&\frac{1}{2\sigma_{k,n}^2}z_{k,n}^2\zeta_{k,n}\left\|W_{k,n}\right\|^2 + \frac{\sigma_{k,n}^2}{2} + \frac{z_{k,n}^2}{2} + \frac{\bar{\varepsilon}_{k,n}^2}{2}\end{aligned} \tag{3.34}$$

where $\zeta_{k,n} = \left\|\psi_{k,n}\right\|^2$, $\sigma_{k,n}$ is a positive constant to be designed, and $\left|\varepsilon_{k,n}\right| \le \bar{\varepsilon}_{k,n}$ represents the approximate error, $\bar{\varepsilon}_{k,n} > 0$.

By incorporating (3.32)–(3.34) into (3.31) yields

$$\begin{aligned}\dot{V}_{k,n} \le&\dot{V}_{k,n-1} + z_{k,n}\sum_{b=1}^{Z} l_{k,b}\left(\bar{u}_{k,b}\rho_{k,b} + c_{k,b}\right) + \frac{1}{2\sigma_{k,n}^2}z_{k,n}\hat{\zeta}_{k,n}\left\|W_{k,n}\right\|^2 + \frac{z_{k,n}^2}{2} - \frac{z_{k,n-1}^2}{2}\\ &- \frac{1}{r_{k,n}}\tilde{\zeta}_{k,n}\left(\dot{\hat{\zeta}}_{k,n} - \frac{1}{2\sigma_{k,n}^2}r_{k,n}z_{k,n}^2\left\|W_{k,n}\right\|^2\right) + \frac{\sigma_{k,n}^2}{2} + \frac{\bar{\varepsilon}_{k,n}^2}{2} - z_{k,n}z_{k,n-1}.\end{aligned} \tag{3.35}$$

The ETM of relative threshold is designed as follows

$$\varpi_{k,b} = -(1+\eta)\left[\tilde{u}_{k,b}\tanh\left(\frac{z_{k,n}sgn(l_{k,b})\tilde{u}_{k,b}}{\lambda}\right) + \gamma\tanh\left(\frac{z_{k,n}sgn(l_{k,b})\gamma}{\lambda}\right)\right], \tag{3.36}$$

$$\begin{cases}\bar{u}_{k,b}(t) = \varpi_{k,b}\left(t_{k,F}\right), \quad t_{k,F} \le t < t_{k,F+1}\\ t_{i,F+1} = \inf\left\{t \in R|\left|E_{k,b}(t)\right| \ge \eta\left|\bar{u}_{k,b}(t)\right| + \eta_1\right\}\end{cases} \tag{3.37}$$

where $0 < \eta < 1$, $\lambda > 0$, and $\gamma > 0$ are design constants; $E_{k,b}(t) = \bar{u}_{k,b}(t) - \varpi_{k,b}(t)$, in which $\bar{u}_{k,b}(t)$ denotes the control signal and $\varpi_{k,b}(t)$ is the event-triggered control input; and $\gamma > \eta_1/(1-\eta)$ and $m \in Z^+$. When the trigger condition $\left|E_{k,b}(t)\right| \geq \eta \left|\bar{u}_{k,b}(t)\right| + \eta_1$ holds true, $\bar{u}_{k,b}(t) = \varpi_{k,b}\left(t_{k,F}\right)$ is updated and keeps this value until the next event is triggered. $t_{k,F}$ denotes the moment when the event is triggered, $t_{k,F} > 0$, and $F \in Z^+$. The control law $\tilde{u}_{k,b}$ will be designed later.

For any $t \in [t_{k,F}, t_{k,F+1})$, $\varpi_{k,b}(t) = (1 + \eta\phi_1(t))\,\bar{u}_{k,b}(t) + \eta_1\phi_2(t)$, in which $|\phi_1(t)| \leq 1$ and $|\phi_2(t)| \leq 1$. Thereby, it can be further articulated as

$$\bar{u}_{k,b}(t) = \frac{\varpi_{k,b}(t) - \eta_1\phi_2(t)}{1 + \eta\phi_1(t)}. \tag{3.38}$$

Based on the uncertain actuator model and ETM, the control law $\tilde{u}_{k,b}$ is constructed as follows

$$\tilde{u}_{k,b} = sgn(l_{k,b})K_{k,b}^T H \tag{3.39}$$

where $K_{k,b} = [K_{k,b11}, K_{k,b21}, \ldots, K_{k,b2Z}]^T$, $K_{k,b11} = \frac{1}{\sum_{b=1,b\in L_{m1}}^{Z} |l_{k,b}|\rho_{k,b}}$, and $H = [\alpha_{k,n}, 1, \ldots, 1]^T$. Especially, if $b \in L_{m2}$, one has $K_{k,b2Z} = -\frac{|l_{k,b}|c_{k,b}}{\sum_{b=1,b\in L_{m1}}^{Z} |l_{k,b}|\rho_{k,b}}$. In contrast, if $b \in L_{m1}$, one has $K_{k,b2Z} = 0$.

Further, it can be inferred that

$$\sum_{b=1,b\in L_{m1}}^{Z} z_{k,n}|l_{k,b}|\rho_{k,b}K_{k,b}^T H_{k,b} + \sum_{b=1,b\in L_{m2}}^{Z} z_{k,n}|l_{k,b}|c_{k,b} = z_{k,n}\alpha_{k,n}. \tag{3.40}$$

Remark 2. *It is noteworthy that, from Equations* (3.39)–(3.40)*, it can be observed that $\rho_{k,b}$ and $c_{k,b}$ are all unknown constants. Therefore, the value of $K_{k,b}$ cannot be directly measured. To achieve the feasibility of the intermediate control law $\tilde{u}_{k,b}$, the estimation $\hat{K}_{k,b}$ is utilized to estimate the value of $K_{k,b}$, resulting in an estimation error $\tilde{K}_{k,b} = K_{k,b} - \hat{K}_{k,b}$.*

Then, $\tilde{u}_{k,b}$ is re-expressed as

$$\tilde{u}_{k,b} = sgn(l_{k,b})\hat{K}_{k,b}^T H. \tag{3.41}$$

According to (3.36), (3.38), and **Lemma 1**, it can be obtained that

$$\begin{aligned}
z_{k,n}sgn(l_{k,b})\bar{u}_{k,b} =& - z_{k,n}sgn(l_{k,b})\left(\frac{1+\eta}{1+\phi_1\eta}\left(\tilde{u}_{k,b}\tanh\left(\frac{z_{k,n}sgn(l_{k,b})\tilde{u}_{k,b}}{\lambda}\right)\right.\right.\\
&\left.\left. + \gamma\tanh\left(\frac{z_{k,n}sgn(l_{k,b})\gamma}{\lambda}\right)\right) + \frac{\phi_2\eta_1}{1+\phi_1\eta_1}\right)\\
\leq& \left|z_{k,n}sgn(l_{k,b})\tilde{u}_{k,b}\right| - z_{k,n}sgn(l_{k,b})\tilde{u}_{k,b}\tanh\left(\frac{z_{k,n}sgn(l_{k,b})\tilde{u}_{k,b}}{\lambda}\right)\\
&+ \left|z_{k,n}sgn(l_{k,b})\gamma\right| - z_{k,n}sgn(l_{k,b})\gamma\tanh\left(\frac{z_{k,n}sgn(l_{k,b})\gamma}{\lambda}\right) - \left|z_{k,n}sgn(l_{k,b})\tilde{u}_{k,b}\right|\\
\leq& z_{k,n}sgn(l_{k,b})\tilde{u}_{k,b} + 0.557\lambda.
\end{aligned} \tag{3.42}$$

By incorporating (3.38)–(3.42) into (3.35) yields

$$\begin{aligned}\dot{V}_{k,n} \leq & \dot{V}_{k,n-1} + \sum_{b=1,b\in L_{m1}}^{Z} z_{k,n}|l_{k,b}|sng(l_{k,b})\rho_{k,b}\tilde{u}_{k,b} + 0.557\sum_{b=1,b\in L_{m1}}^{Z}|l_{k,b}|\rho_{k,b}\lambda \\ & + \sum_{b=1,b\in L_{m2}}^{Z} z_{k,n}l_{k,b}c_{k,b} - z_{k,n}z_{k,n-1} + \frac{1}{2\sigma_{k,n}^2}z_{k,n}\hat{\zeta}_{k,n}\left\|W_{k,n}\right\|^2 + \frac{z_{k,n}^2}{2} - \frac{z_{k,n}^2}{2} \\ & - \frac{1}{r_{k,n}}\tilde{\zeta}_{k,n}\left(\dot{\hat{\zeta}}_{k,n} - \frac{1}{2\sigma_{k,n}^2}r_{k,n}z_{k,n}^2\left\|W_{k,n}\right\|^2\right) + \sum_{q=1}^{n}\left(\frac{\sigma_{k,q}^2}{2} + \frac{\bar{\varepsilon}_{k,q}^2}{2}\right) \\ \leq & \dot{V}_{k,n-1} + z_{k,n}\left(\alpha_{k,n} + \frac{1}{2\sigma_{k,n}^2}z_{k,n}\hat{\zeta}_{k,n}\left\|W_{k,n}\right\|^2\right) - \frac{z_{k,n}^2}{2} - z_{k,n}z_{k,n-1} \\ & - \frac{1}{r_{k,n}}\tilde{\zeta}_{k,n}\left(\dot{\hat{\zeta}}_{k,n} - \frac{1}{2\sigma_{k,n}^2}r_{k,n}z_{k,n}^2\left\|W_{k,n}\right\|^2\right) + \frac{z_{k,n}^2}{2} + \sum_{q=1}^{n}\left(\frac{\sigma_{k,q}^2}{2} + \frac{\bar{\varepsilon}_{k,q}^2}{2}\right) \\ & - \sum_{b=1,b\in L_{m1}}^{Z}|l_{k,b}|\tilde{K}_{k,b}^T\rho_{k,b}\Gamma_{k,b}^{-1}\left(\dot{\hat{K}}_{k,b} + z_{k,n}\Gamma_{k,b}H\right) + 0.557\sum_{b=1,b\in L_{m1}}^{Z}|l_{k,b}|\rho_{k,b}\lambda. \end{aligned} \tag{3.43}$$

$\dot{\hat{\zeta}}_{k,n}$, $\dot{\hat{K}}_{k,b}$, and $\alpha_{k,n}$ are designed as

$$\dot{\hat{\zeta}}_{k,n} = \frac{1}{2\sigma_{k,n}^2}r_{k,n}z_{k,n}^2\left\|W_{k,n}\right\|^2 - \xi_{k,n}\hat{\zeta}_{k,n}, \tag{3.44}$$

$$\dot{\hat{K}}_{k,b} = -z_{k,n}\Gamma_{k,b}H - g_{k,b}\Gamma_{k,b}\hat{K}_{k,b}, \tag{3.45}$$

$$\alpha_{k,n} = -\beta_{k,n}z_{k,n} - \frac{1}{2\sigma_{k,n}^2}z_{k,n}\hat{\zeta}_{k,n}\left\|W_{k,n}\right\|^2. \tag{3.46}$$

Substituting (3.44)–(3.46), one has

$$\begin{aligned}\dot{V}_{k,n} \leq & -\Delta_n\left\|e_k\right\|^2 + M_1 - \sum_{q=1}^{n}\beta_{k,q}z_{k,q}^2 + \sum_{q=1}^{n}\frac{1}{r_{k,q}}\xi_{k,q}\tilde{\zeta}_{k,q}\hat{\zeta}_{k,q} + \sum_{q=1}^{n}\left(\frac{\sigma_{k,q}^2}{2} + \frac{\bar{\varepsilon}_{k,q}^2}{2}\right) \\ & + \sum_{b=1,b\in L_{m1}}^{Z}|l_{k,b}|\rho_{k,b}g_{k,b}\tilde{K}_{k,b}^T\hat{K}_{k,b} + 0.557\sum_{b=1,b\in L_{m1}}^{Z}|l_{k,b}|\rho_{k,b}\lambda + \frac{z_{k,n}^2}{2} \end{aligned} \tag{3.47}$$

where $\Delta_n = \Delta_{n-1} - 1$.

Utilizing Young's inequality yields

$$\sum_{q=1}^{n}\frac{1}{r_{k,q}}\xi_{k,q}\tilde{\zeta}_{k,q}\hat{\zeta}_{k,q} \leq -\sum_{q=1}^{n}\frac{1}{2r_{k,q}}\xi_{k,q}\tilde{\zeta}_{k,q}^2 + \sum_{q=1}^{n}\frac{1}{2r_{k,q}}\xi_{k,q}\zeta_{k,q}^2, \tag{3.48}$$

$$|l_{k,b}|\rho_{k,b}g_{k,b}\tilde{K}_{k,b}^T\hat{K}_{k,b} \leq -\frac{1}{2}|l_{k,b}|\rho_{k,b}g_{k,b}\tilde{K}_{k,b}^T\tilde{K}_{k,b} + \frac{1}{2}|l_{k,b}|\rho_{k,b}g_{k,b}K_{k,b}^TK_{k,b}. \tag{3.49}$$

Further, combining (3.47)–(3.49) yields

$$\dot{V}_{k,n} \leq -\Delta_n \|e_k\|^2 - \sum_{q=1}^{n} \beta_{k,q} z_{k,q}^2 - \sum_{q=1}^{n} \frac{1}{2r_{k,q}} \xi_{k,q} \tilde{\zeta}_{k,q}^2 - \sum_{b=1,b\in L_{m1}}^{Z} \frac{1}{2} |l_{k,b}| \rho_{k,b} g_{k,b} \tilde{K}_{k,b}^T \tilde{K}_{k,b} + \frac{z_{k,n}^2}{2} + \Omega \tag{3.50}$$

where $\Omega = M_1 + \sum_{q=1}^{n} \frac{1}{2r_{k,q}} \xi_{k,q} \zeta_{k,q}^2 + \sum_{b=1,b\in L_{m1}}^{Z} \frac{1}{2} |l_{k,b}| \rho_{k,b} g_{k,b} K_{k,b}^T K_{k,b} + 0.557 \sum_{b=1,b\in L_{m1}}^{Z} |l_{k,b}| \rho_{k,b} \lambda + \sum_{q=1}^{n} \left(\frac{\sigma_{k,q}^2}{2} + \frac{\bar{\varepsilon}_{k,q}^2}{2} \right)$.

Ultimately, it can be given as follows

$$\begin{aligned} \dot{V}_{k,n} \leq & -\mu_1 e_k^T O_k e_k - \mu_2 \sum_{q=1}^{n-1} \frac{1}{2} z_{k,q}^2 - \mu_3 \frac{1}{2} z_{k,n}^2 - \mu_4 \sum_{q=1}^{n} \frac{1}{2r_{k,q}} \tilde{\zeta}_{k,q}^2 \\ & - \mu_5 \sum_{b=1,b\in L_{m1}}^{Z} \frac{1}{2} |l_{k,b}| \rho_{k,b} \tilde{K}_{k,b}^T \Gamma_{k,b}^{-1} \tilde{K}_{k,b} + \Omega, \end{aligned} \tag{3.51}$$

where $\mu_1 = \min\left\{\frac{2\Delta_n}{\lambda_{max}(O_k)}\right\}$, $\mu_2 = \min\left\{2\beta_{k,q}\right\}$, $\mu_3 = \min\{2\beta_{k,n} - 1\}$, $\mu_4 = \min\left\{\xi_{k,q}\right\}$, and $\mu_5 = \min\left\{\frac{g_{k,b}}{\lambda_{max}(\Gamma_{k,b}^{-1})}\right\}$. $\lambda_{max}(O_k^{-1})$ and $\lambda_{max}(\Gamma_{k,b}^{-1})$ are the maximum eigenvalues of O_k^{-1} and $\Gamma_{k,b}^{-1}$, respectively.

Hence, it could be obtained that

$$\dot{V}_{k,n} \leq -\mu_6 V_{k,n} + \Omega \tag{3.52}$$

where $\mu_6 = \min\{\mu_1, \mu_2, \mu_3, \mu_4, \mu_5\}$. The proposed control method can be showed by Figure 1.

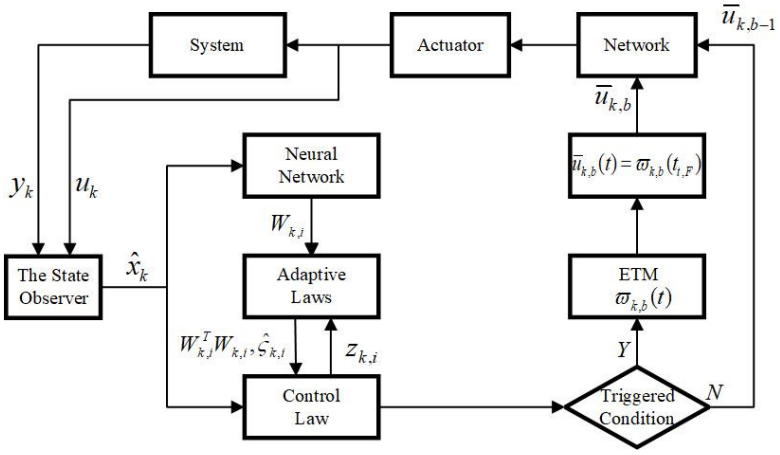

Figure 1. A framework for uncertain nonlinear MASs tracking control under actuator failures.

3.3. Stability analysis

Theorem 1. *Under the **Lemma 1**, **Assumption 1** and **Assumption 2**, combining the MASs (2.1) with virtual control laws (3.15), (3.26), (3.46) and adaptive laws (3.16), (3.27), (3.44), (3.45) designed based on the ETM (3.36), (3.37) and the state observer (3.1), the following conditions are satisfied:*

1) All signals within the closed-loop system remain bounded, with each agents' output following the trajectory of the virtual leader;

2) The occurrence of Zeno's phenomenon can be successfully prevented.

Proof: Multiplying both sides of Equation (3.52) by $e^{\mu_6 t}$ simultaneously yields

$$\frac{d(V_{k,n}e^{\mu_6 t})}{dt} \leq \Omega e^{\mu_6 t}. \tag{3.53}$$

Then, solving the differential equation gives

$$\frac{1}{2}z_{k,1}^2 \leq V_{k,n}(t) \leq e^{-\mu_6 t}V_k, n(0) + \frac{\Omega}{\mu_6}(1 - e^{-\mu_6 t}). \tag{3.54}$$

Thus, $z_{k,1}^2$ converges exponentially to the tight set $\Xi = \left\{z_{k,1}|z_{k,1}^2 \leq \frac{2\Omega}{\mu_6}\right\}$ at the rate of μ_6 and can be tuned by adjusting the design parameters for Ξ.

According to the tight set Ξ it follows that the error signals are all bounded, and y_s is bounded, and $\zeta_{k,1}$ is a constant so that $x_{k,1}$, $\tilde{\zeta}_{k,1}$, and e_k are also bounded. Further, the bound of (3.7), (3.15), (3.26), and (3.46) yields that $\alpha_{l,1}$, and $x_{k,2}$ are all bounded. Similarly, $x_{k,i}$, $\hat{\zeta}_{k,1}$, $\hat{x}_{k,i}$ and $\alpha_{k,i}$ are all bounded. Moreover, because $\tilde{K}_{k,b} = K_{k,b} - \hat{K}_{k,b}$ and $\tilde{K}_{k,b}$ are bounded, $\hat{K}_{k,b}$ is also bounded. Thus, all signals within the closed-loop system are semi-global consistent and eventually bounded.

Based on the literature [35], defining the synchronization error vector $\Theta_k = [z_{1,1}, z_{2,1}, ..., z_{k,1}]^T$, one has:

$$\left\|\bar{\Theta}_k\right\| \leq \frac{\|\Theta_k\|}{\lambda_{max}(L + A)} \tag{3.55}$$

where $\bar{\Theta}_k = [\bar{z}_{1,1}, \bar{z}_{2,1}, ..., \bar{z}_{k,1}]^T = Y_k - y_s$, $Y_k = [y_{1,1}, y_{2,1}, ..., y_{k,1}]^T$, $y_s = [y_{s1}, y_{s2}, ..., y_{sn}]^T$, $\lambda_{max}(L + A)$ denotes $(L + A)$ the maximum eigenvalue. Thus, the tracking error of the MASs converges to the following set:

$$\left|\bar{z}_{k,n}\right| \leq min\left\{\frac{\sqrt{2}}{\lambda_{max}(L + A)}\left(\frac{\Omega}{\mu_6}\right)^{\frac{1}{2}}\right\}. \tag{3.56}$$

(3.28), as well as $t \in [t_{k,F}, t_{k,F+1})$, yields

$$\frac{d|E_{k,b}|}{dt} = sgn(E_{k,b})\dot{E}_{k,b} \leq |\dot{\varpi}_{k,b}|. \tag{3.57}$$

Expressed by (3.38), $\dot{\varpi}_{k,b}$ remains continuously bounded with the existence of a constant $\bar{\varpi}_{k,b} > 0$ ensuring, $|\dot{\varpi}_{k,b}| < \bar{\varpi}_{k,b}$. Furthermore, it can be found that $lim_{t_{k,m}\to t_{k,m+1}}E_{k,b}(t) = \eta|\bar{u}_{k,b}(t)| + \eta_1$. According to the Lagrange mean value theorem, it can be obtained that:

$$t_{k,F+1} - t_{k,F} \geq \frac{\eta|\bar{u}_{k,b}(t)| + \eta_1}{\bar{\varpi}_{k,b}}. \tag{3.58}$$

Since $t_{k,F+1} - t_{k,F} \geq t^\diamond$, $t^\diamond$ should be guaranteed to satisfy $t^\diamond \geq \frac{\eta|\bar{u}_{k,b}(t)|+\eta_1}{\bar{\varpi}_{k,b}}$. Obviously, the considered system can effectively avoid the Zeno behavior.

Remark 3. *Zeno's phenomenon involves an infinite number of events occurring in a finite period of time, resulting in a system requiring an infinite update. This may aggravate the computational weight of the system, making real-time control unattainable, further leading to communication overload, and possibly even causing system crashes or performance degradation. Therefore, designing event-triggered control systems that exclude the Zeno phenomenon ensures that the system maintains computational feasibility, communication efficiency, and utility in long-term operation while maintaining the desired performance and reliability.*

Remark 4. *Further analysis reveals that* $|z_{k,1}| \leq \max\left\{(2V_{k,n}(0))^{\frac{1}{2}}, \left(\frac{2\Omega}{\mu_6}\right)^{\frac{1}{2}}\right\}$. *It is evident that the set can be adjusted by selecting the parameters to be designed, such as* $\beta_{k,q}$, $\beta_{k,n}$, $\xi_{k,q}$, $g_{k,b}$, *and so on. Additionally, from Eqs* (3.50)–(3.54)*, it can be observed that when* $\rho_{k,b}$ *remains constant, the residual set varies with the changes in* $c_{k,b}$. *Similarly, when* $c_{k,b}$ *remains constant,* Ω *increases with the rising of* $\rho_{k,b}$, *resulting in an expansion of the residual set of tracking errors.* □

4. Simulation example and analysis

This section aims to validate the control method's efficacy by conducting a comprehensive analysis of numerical and practical examples.

4.1. Numerical example

Consider a MAS with actuator failures comprising a virtual leader and three follower agents. The communication topology is illustrated in Figure 2, and the model for the follower agents are detailed as

$$\begin{cases} \dot{x}_{k,1} = x_{k,2} + f_{k,1}(X_{k,1}) \\ \dot{x}_{k,2} = \sum_{b=1}^{2} l_{k,b}u_{k,b} + f_{k,2}(X_{k,2}) \\ y_k = x_{k,1} \end{cases} \tag{4.1}$$

where $k = 1, 2, 3$ and selecting the nonlinear functions as $f_{k,1} = 0.1(1 + sin^2(x_{k,1}))x_{k,1}$ and $f_{k,2} = 2.5x_{k,2} + x_{k,1}x_{k,2}^2$; $u_{k,b} = \rho_{k,b}\bar{u}_{k,b} + c_{k,b}$, $l_{k,b} = 1(b = 1, 2)$ unknown constants and $u_{k,1}$ and $u_{k,2}$ are represent system input signals. $x_{k,1}(0) = x_{k,2}(0) = 0.1$ are initial states and the initial values of the state observer estimated are $\hat{x}_{k,1}(0) = \hat{x}_{k,2}(0) = 0.2$. The desired tracking signal is $y_s = sin(2t)$.

The basis function for RBFNNs is designed as follows:

$$W_{k,i}(X_{k,i}) = -\exp\left(\frac{(X_{k,i} - p_i)^T(X_{k,i} - p_i)}{\kappa_i^2}\right) \tag{4.2}$$

where $i = 1, 2, \ldots, 16$; the Gaussian function centered at κ_i has a distribution interval in $[-1, 1]$.

Other correlated parameters to be designed as $\eta = 0.2$, $\lambda = 0.5$, $\eta_1 = 0.2$, $\gamma = \eta_1/(1 - \eta) + 0.01$, $\sigma_{k,1} = \sigma_{k,2} = r_{k,1} = r_{k,2} = \xi_{k,1} = \xi_{k,2} = 0.1$, $h_{k,1} = 120$, $h_{k,2} = 60^2$, $\beta_{k,1} = 37$, $\beta_{k,2} = 18$, $g_{k,b} = 0.3$, $\Gamma_{k,b} = [1, 0; 0, 1]$, $\hat{K}_{k,b}(0) = [0, 0, 0]^T$, and $\hat{\zeta}_{k,1}(0) = \hat{\zeta}_{k,2}(0) = 0$.

Consider the cases of two actuator failures, which are shown as follows. Case 1: Actuator 1 of each agent keeps operating normally, and Actuator 2 of each agent loses 30% of performance after $t = 8s$. Case 2: Each agent's Actuator 1 fails 20% of the faults throughout the run and each agent's Actuator 2 fails completely.

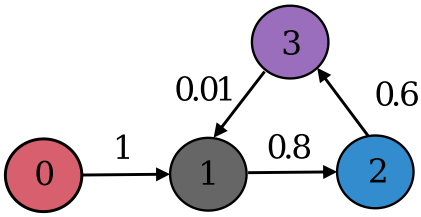

Figure 2. Topology of communication graph.

The simulation results from Figure 3 to Figure 8 indicate that all signals are bounded. From Figures 3(a) and 4(a), it can be observed that when facing actuator failures, every agent's output can effectively track the output signal of the virtual leader, enabling MASs to achieve signal synchronization. Figures 4 and 7 show the values of observer state and real state for two cases, with small error values between them. In Figures 5 and 8, it is evident that whether the actuator partially fails or a complete failure occurs after 8 seconds of normal operation, the updated control signal will be delivered to the system upon satisfying the event-triggered condition. This serves as compensation for the actuator failures, demonstrating the better effectiveness of the proposed control method on the system. By observing Figure 3(c), it significantly exceeds the simulation time step of 0.01s, indicating the absence of the Zeno phenomenon. The values in Table 1 elucidate that the two cases conserve a maximum of 72.60% and 77.60% of communication resources, respectively. This illustrates that, in contrast to traditional TTM, ETM offers significant conservation of communication resources.

The designed control method is compared with the method in the literature [24] to compare its tracking performance in the uncertain nonlinear MASs with actuator failures. From Figures 3 and 4, it can be observed that the designed state observer is effective in estimating the system state and the tracking error of each agent converges quickly to the range of the ± 0.05 error band within $0.2s$. The tracking performance is better than that of the literature [24], and there is no need to assume in advance that the system state is measurable at the time. Therefore, the designed control method is more general.

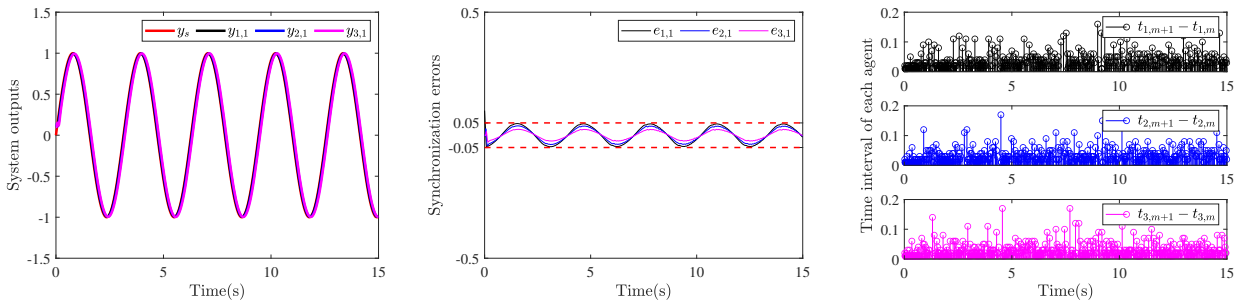

(a) (b) (c)

Figure 3. Example 1: Case 1 about (a)System outputs and desired output y_s. (b) Synchronization errors. (c) Time intervals.

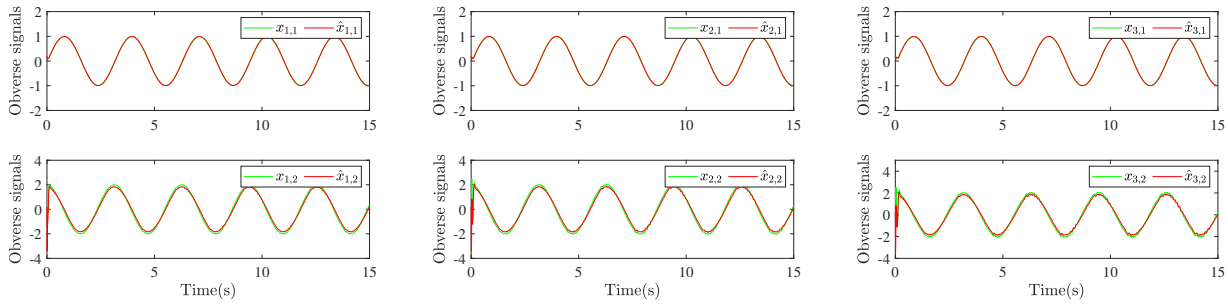

Figure 4. Example 1: Case 1 about the values of real states $x_{k,i}$ and state observer estimated $\hat{x}_{k,i}$.

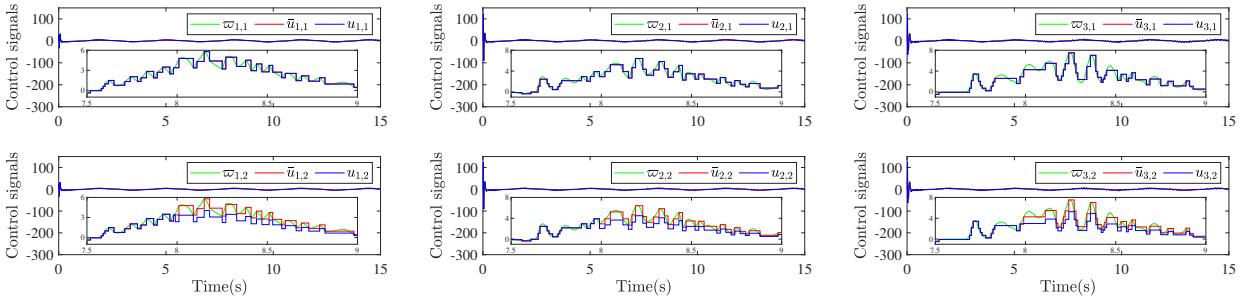

Figure 5. Example 1: Case 1 about the event-triggered control input $\varpi_{k,b}$, actuator input $\bar{u}_{k,b}$, and system input $u_{k,b}$.

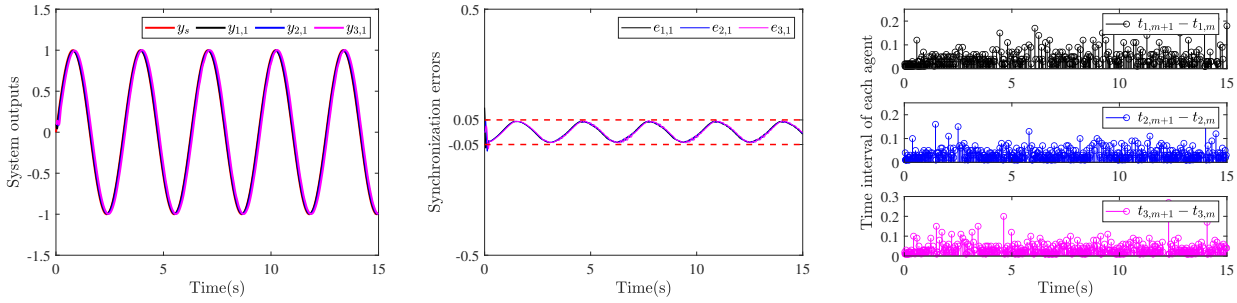

Figure 6. Example 1: Case 2 about (a)System outputs and desired output y_s. (b) Synchronization errors. (c) Time intervals.

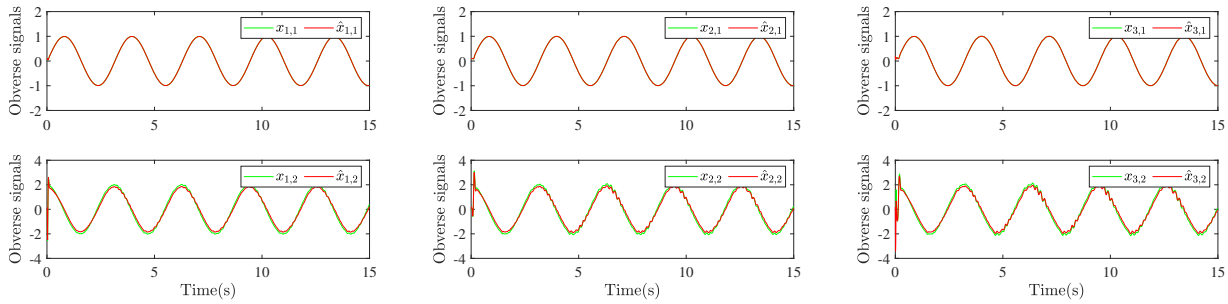

Figure 7. Example 1: Case 2 about the values of real states $x_{k,i}$ and state observer estimated $\hat{x}_{k,i}$.

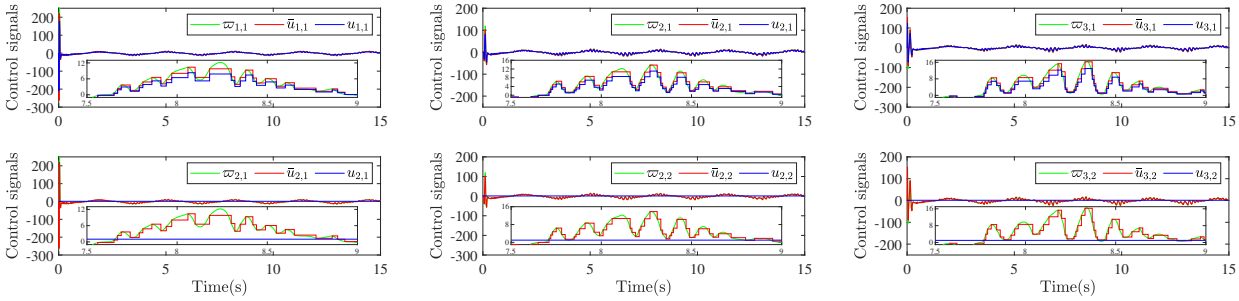

Figure 8. Example 1: Case 2 about the event-triggered control input $\varpi_{k,b}$, actuator input $\bar{u}_{k,b}$, and system input $u_{k,b}$.

4.2. Practical example

To assess the proposed control approach in the actual system effectiveness, reference [35] for the multi-single-link robotic arm system ($k = 1, 2, 3$)

$$\begin{cases} \dot{x}_{k,1} = x_{k,2} \\ \dot{x}_{k,2} = \sum_{b=1}^{2} l_{k,b}u_{k,b} - \frac{1}{J}(Bx_{k,2} + mglsin(x_{k,1})) \\ y_k = x_{k,1} \end{cases} \tag{4.3}$$

where $f_{k,2} = -\frac{1}{J}(Bx_{k,2} + mglsin(x_{k,1}))$ denotes the unknown smooth nonlinear functions; $u_{k,b} = \rho_{k,b}\bar{u}_{k,b} + c_{k,b}$, $l_{k,b} = 1(b = 1, 2)$ are unknown constants; and $u_{k,1}$ and $u_{k,2}$ represent system input signals. $x_{k,1}(0) = x_{k,2}(0) = 0.1$ are initial states, representing joint angle and angular velocity, respectively and the initial values of the state observer's estimated state are $\hat{x}_{k,1}(0) = \hat{x}_{k,2}(0) = 0.2$. The robotic arm system parameters are specified as follows: $J = 0.8$, $B = 1$ and $mgl = 10$. The desired tracking signal is $y_s = sin(2t)$.

The communication topology graph and the selection of the basis functions for the cases of actuator failures are the same as for the numerical example. The other relevant parameters to be designed are as follows: $\eta = 0.1$, $\lambda = 3$, $\eta_1 = 0.5$, $\gamma = \eta_1/(1-\eta)+0.001$, $\sigma_{k,1} = \sigma_{k,2} = r_{k,1} = r_{k,2} = 0.1$, $\xi_{k,1} = \xi_{k,2} = 0.5$, $h_{k,1} = 112$, $h_{k,2} = 56^2$, $\beta_{k,1} = 44$, $\beta_{k,2} = 16$, $g_{k,b} = 0.01$, $\Gamma_{k,b} = [1, 0; 0, 1]$, $\hat{K}_{k,b}(0) = [0, 0, 0]^T$ and $\hat{\zeta}_{k,1}(0) = \hat{\zeta}_{k,2}(0) = 0$.

Figure 9 to Figure 14 and Table 1 show the simulation results of the multi-single-link robotic arm system (4.3), which is analyzed similarly to the numerical simulation. By utilizing the proposed control method, the multi-single-link robotic arm system achieves the desired tracking performance and signal bound while synchronizing the signals in the case of actuator failures subjected to the two cases respectively. Furthermore, the nonexistence of the Zeno phenomenon is guaranteed.

Table 1. Saving percentage in communication resources for Examples.

Example	Cases	Agent 1	Agent 2	Agent 3
Example 1	Case 1	72.53%	68.33%	63.20%
	Case 2	77.60%	69.20%	69.26%
Example 2	Case 1	62.20%	61.66%	63.73%
	Case 2	61.66%	62.40%	65.60%

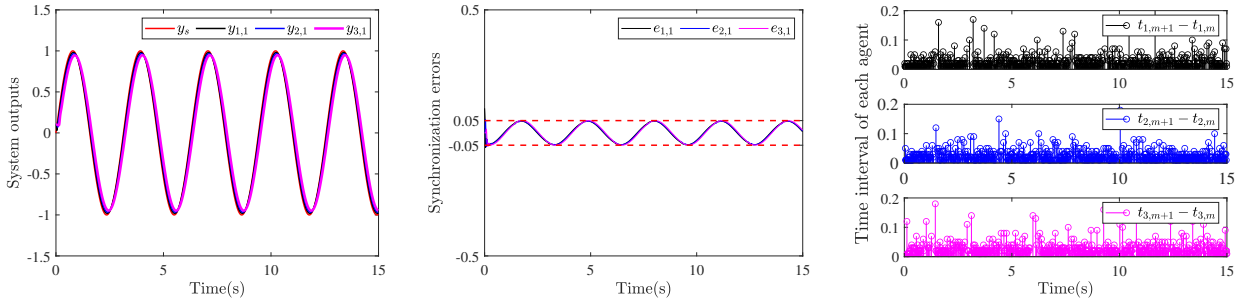

Figure 9. Example 2: Case 1 about (a)System outputs and desired output y_s. (b) Synchronization errors. (c) Time intervals.

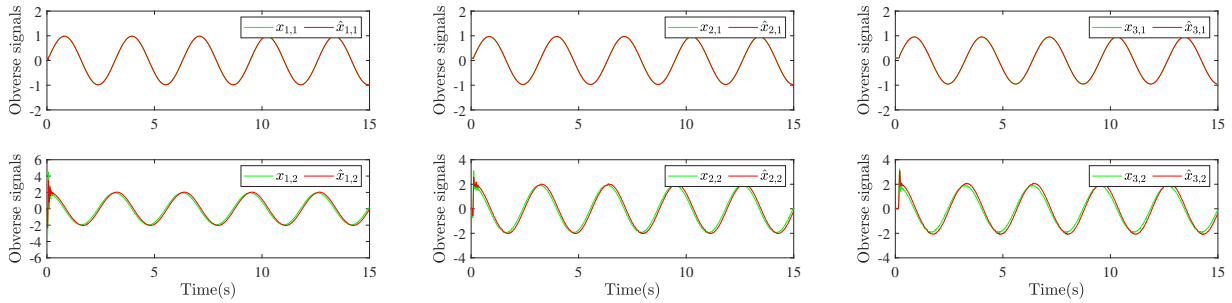

Figure 10. Example 2: Case 1 about the values of real states $x_{k,i}$ and state observer estimated $\hat{x}_{k,i}$.

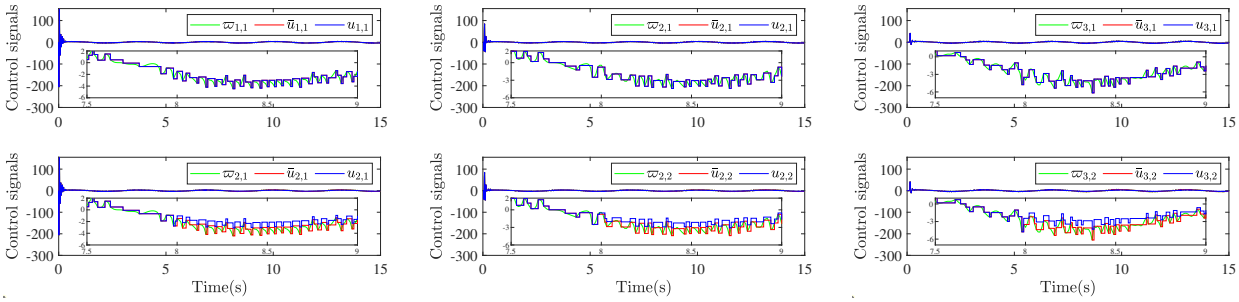

Figure 11. Example 2: Case 1 about the event-triggered control input $\varpi_{k,b}$, actuator input $\bar{u}_{k,b}$, and system input $u_{k,b}$.

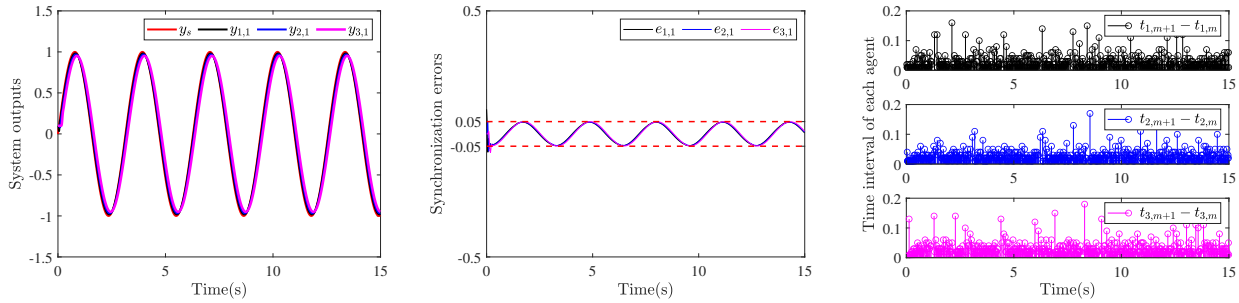

(a) (b) (c)

Figure 12. Example 2: Case 2 about (a) System outputs and desired output y_s. (b) Synchronization errors. (c) Time intervals.

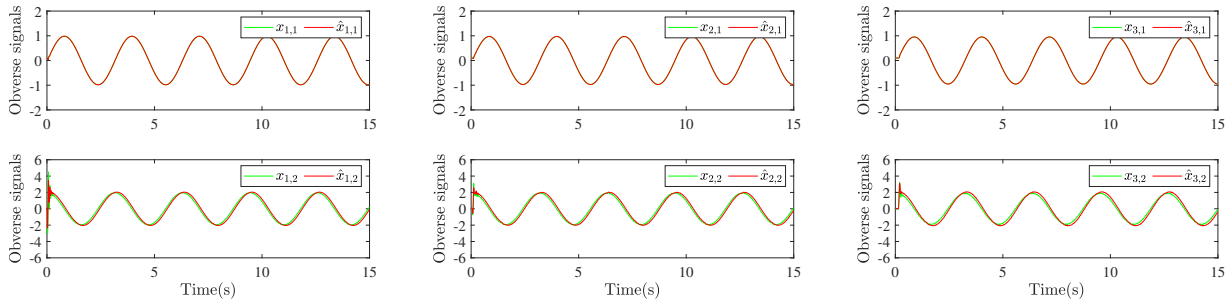

Figure 13. Example 2: Case 2 about the values of real states $x_{k,i}$ and state observer estimated $\hat{x}_{k,i}$.

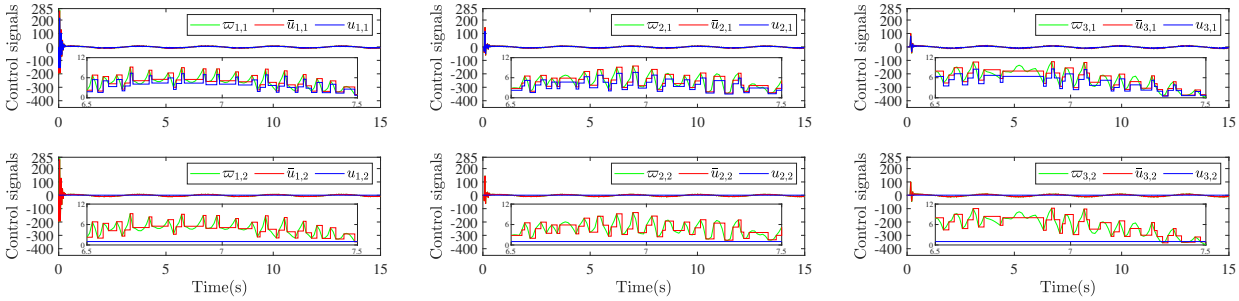

Figure 14. Example 2: Case 2 about the event-triggered control input $\varpi_{k,b}$, actuator input $\bar{u}_{k,b}$, and system input $u_{k,b}$.

5. Conclusions

This research is targeted at a class of uncertain nonlinear MASs with actuator failures, whose control objective is to design an adaptive NNs event-triggered consensus control method with state observers to estimate unmeasurable states of the MASs, in order to realize the dynamic compensation of actuator failures while reducing the communication resources among the agents and avoiding Zeno phenomenon, and to make the all follower synchronization. Finally, the simulation results show the effectiveness of the control method. In future work, we will utilize the proposed method in combination with a fixed-time disturbance observer, speeding up the convergence of the system as well as directly measuring the disturbance signals, which is a valuable research work.

Author contributions

Kairui Chen: Conceptualization, methodology, investigation, writing - review and editing, validation, project administration; Yongping Du: methodology, Methodology, software, formal analysis, writing-review and editing, methodology; Shuyan Xia: Supervision, project administration, writing - review and editing, validation. All authors have read and approved the final version of the manuscript for publication.

Use of AI tools declaration

The authors declare they have not used Artificial Intelligence (AI) tools in the creation of this article.

Acknowledgments

This work was supported in part by the National Natural Science Foundation of China (62103115, 52075108), in part by the Scientific and Technological Research Program of Chongqing Municipal Education Commission (KJZD-K202301203), in part by the Scientific and Technological Research Program of Wanzhou District(wzstc-20230309), in part by the Multi-dimensional Data Sensing and Intelligent Information Processing Key Laboratory Open Foundation (DWSJ2306), and in part by the Science and Technology Research Program of Guangzhou (2024404T9895, SL2023A04J00530).

Conflict of interest

The authors declare that they have no known competing financial interests or personal relationships that could have appeared to influence the work reported in this paper.

References

1. M. Shahriari-kahkeshi, N. Meskin, Adaptive cooperative control of nonlinear multi-agent systems with uncertain time-varying control directions and dead-zone nonlinearity, *Neurocomputing*, **464** (2021), 151–163. https://doi.org/10.1016/j.neucom.2021.08.065
2. X. D. Li, Y. Z. Lv, G. H. Wen, X. H. Yu, Tracking consensus of multi-agent systems with varying number of agents under actuator attacks, *IEEE Trans. Circuits Syst. II*, **70** (2023), 4514–4518. https://doi.org/10.1109/TCSII.2023.3289847
3. M. Z. Xia, Z. C. Liu, T. P. Zhang, Distributed adaptive cooperative control via command filters for multi-agent systems including input unmodeled dynamics and sensor faults, *Appl. Math. Comput.*, **457** (2023), 128194. https://doi.org/10.1016/j.amc.2023.128194
4. G. L. Xiao, J. R. Wang, D. Shen, Adaptive fixed-time consensus for stochastic multi-agent systems with uncertain actuator faults, *ISA Trans.*, **137** (2023), 369–378. https://doi.org/10.1016/j.isatra.2023.01.003
5. J. X. Chen, J. M. Li, S. Y. Liu, A. L. Zhao, Adaptive neural consensus of nonlinearly parameterized multi-agent systems with periodic disturbances, *ISA Trans.*, **126** (2022), 160–170. https://doi.org/10.1016/j.isatra.2021.07.024
6. G. Y. Bao, L. F. Ma, X. J. Yi, Recent advances on cooperative control of heterogeneous multi-agent systems subject to constraints: a survey, *Syst. Sci. Control Eng.*, **10** (2022), 539–551. https://doi.org/10.1080/21642583.2022.2074169
7. J. Sun, J. X. Zhang, L. Liu, Y. M. Wu, Q. H. Shan, Output consensus control of multi-agent systems with switching networks and incomplete leader measurement, *IEEE Trans. Autom. Sci. Eng.*, 2022, 1–10. https://doi.org/10.1109/TASE.2023.3328897
8. W. L. Cheng, K. Zhang, B. Jiang, S. X. Ding, Fixed-fime fault-tolerant formation control for heterogeneous multi-agent systems with parameter uncertainties and disturbances, *IEEE Trans. Circuits Syst. I*, **68** (2021), 2121–2133. https://doi.org/10.1109/TCSI.2021.3061386
9. Z. B. Lin, Z. Liu, C. Y. Su, Y. N. Wang, C. L. P. Chen, Y. Zhang, Adaptive fuzzy prescribed performance output-feedback cooperative control for uncertain nonlinear multiagent systems, *IEEE Trans. Fuzzy Syst.*, **31** (2023), 4459–4470. https://doi.org/10.1109/TFUZZ.2023.3285649
10. S. C. Tong, M. Xiao, Y. X. Li, Observer-based adaptive fuzzy tracking control for strict-feedback nonlinear systems with unknown control gain function, *IEEE Trans. Cybern.*, **50** (2020), 3903–3913. https://doi.org/10.1109/TCYB.2020.2977175
11. D. Cui, C. K. Ahn, Z. R. Xiang, Fault-tolerant fuzzy observer-based fixed-time tracking control for nonlinear switched systems, *IEEE Trans. Fuzzy Syst.*, **31** (2023), 4410–4420. https://doi.org/10.1109/TFUZZ.2023.3284917

12. G. D. Zong, Y. D. Wang, H. R. Karimi, K. B. Shi, Observer-based adaptive neural tracking control for a class of nonlinear systems with prescribed performance and input dead-zone constraints, *Neural Networks*, **147** (2022), 126–135. https://doi.org/10.1016/j.neunet.2021.12.019

13. X. Y. Chen, F. Zhao, Y. Liu, H. W. Liu, T. W. Huang, J. L. Qiu, Reduced-order observer-based preassigned finite-time control of nonlinear systems and its applications, *IEEE Trans. Syst., Man, Cybern.: Syst.*, **53** (2023), 4205–4215. https://doi.org/10.1109/TSMC.2023.3241365

14. Y. X. Lian, J. W. Xia, J. H. Park, W. Sun, H. Shen, Disturbance observer-based adaptive neural network output feedback control for uncertain nonlinear systems, *IEEE Trans. Neural Networks Learn. Syst.*, **34** (2023), 7260–7270. https://doi.org/10.1109/TNNLS.2021.3140106

15. H. Q. Wang, J. W. Ma, X. D. Zhao, B. Niu, M. Chen, W. Wang, Adaptive fuzzy fixed-time control for high-order nonlinear systems with sensor and actuator faults, *IEEE Trans. Fuzzy Syst.*, **31** (2023), 2658–2668. https://doi.org/10.1109/TFUZZ.2023.3235395

16. C. Sun, Y. Lin, Adaptive output feedback compensation for a class of nonlinear systems with actuator and sensor failures, *IEEE Trans. Syst., Man, Cybern.: Syst.*, **52** (2022), 4762–4771. https://doi.org/10.1109/TSMC.2021.3103908

17. Z. Y. Ma, H. B. Kang, H. J. Ma, Adaptive output-Feedback asymptotic tracking control for a class of nonlinear systems with actuator failure, *J. Franklin Inst.*, **359** (2022), 1881–1898. https://doi.org/10.1016/j.jfranklin.2022.01.037

18. Y. Sun, P. Shi, C. C. Lim, Adaptive consensus control for output-constrained nonlinear multi-agent systems with actuator faults, *J. Franklin Inst.*, **359** (2022), 4216–4232. https://doi.org/10.1016/j.jfranklin.2022.03.025

19. Y. T. Cao, B. Q. Li, S. P. Wen, T. W. Huang, Consensus tracking of stochastic multi-agent system with actuator faults and switching topologies, *Inf. Sci.*, **607** (2022), 921–930. https://doi.org/10.1016/j.ins.2022.06.009

20. J. S. Zhao, Y. Lin, Adaptive actuator failure compensation control: a new scheme based on fault detection and isolation, *IEEE/ASME Trans. Mechatron.*, **28** (2023), 2236–2247. https://doi.org/10.1109/TMECH.2022.3232574

21. Y. Liu, L. Li, Adaptive leader-follower consensus control of multiple flexible manipulators with actuator failures and parameter uncertainties, *IEEE/CAA J. Autom. Sin.*, **10** (2023), 1020–1031. https://doi.org/10.1109/JAS.2023.123093

22. Y. Yang, X. Fan, W. N. Gao, W. B. Yue, A. Liu, S. C. Geng, et al., Event-triggered output feedback control for a class of nonlinear systems via disturbance observer and adaptive dynamic programming, *IEEE Trans. Fuzzy Syst.*, **31** (2023), 3148–3160. https://doi.org/10.1109/TFUZZ.2023.3245294

23. S. Al Issa, I. Kar, Event-triggered adaptive control of uncertain non-linear systems under input delay and limited resources, *Int. J. Dynam. Control*, **9** (2021), 1703–1710. https://doi.org/10.1007/s40435-021-00767-7

24. Y. Wang, Y. H. Yang, L. B. Wu, Adaptive fault-tolerant consensus control of multi-agent systems with event-triggered input, *Inf. Sci.*, **650** (2023), 119594. https://doi.org/10.1016/j.ins.2023.119594

25. J. H. Wang, J. R. Liu, Y. H. Li, C. L. P. Chen, Z. Liu, F. Y. Li, Prescribed time fuzzy adaptive consensus control for multiagent systems with dead-zone input and sensor faults, *IEEE Trans. Autom. Sci. Eng.*, **21** (2023), 4016–4027. https://doi.org/10.1109/TASE.2023.3291716

26. L. Cao, Q. Zhou, G. W. Dong, H. Y. Li, Observer-based adaptive event-triggered control for nonstrict-feedback nonlinear systems with output constraint and actuator failures, *IEEE Trans. Syst., Man, Cybern.: Syst.*, **51** (2021), 1380–1391. https://doi.org/10.1109/TSMC.2019.2895858

27. Y. X. Li, Z. Hou, W. W. Che, Z. G. Wu, Event-based design of finite-time adaptive control of uncertain nonlinear systems, *IEEE Trans. Neural Networks Learn. Syst.*, **33** (2022), 3804–3813. https://doi.org/10.1109/TNNLS.2021.3054579

28. J. J. Chen, P. Jiang, B. S. Chen, Z. G. Zeng, Adaptive neural event-triggered consensus control for unknown nonlinear second-order delayed multi-agent systems, *Neurocomputing*, **598** (2024), 128067. https://doi.org/10.1016/j.neucom.2024.128067

29. T. T. Chen, B. Niu, J. M. Zhang, D. Wang, Z. H. Wang, Time-/event-triggered adaptive neural asymptotic tracking control of nonlinear interconnected systems with unmodeled dynamics and prescribed performance, *IEEE Trans. Neural Networks Learn. Syst.*, **34** (2023), 6557–6567. https://doi.org/10.1109/TNNLS.2021.3129228

30. J. H. Wang, C. Wang, Z. Liu, C. L. P. Chen, C. L. Zhang, Practical fixed-time adaptive erbfnns event-triggered control for uncertain nonlinear systems with dead-zone constraint, *IEEE Trans. Syst., Man, Cybern.: Syst.*, **54** (2023), 342–351. https://doi.org/10.1109/TSMC.2022.3211658

31. J. H. Wang, Y. C. Yan, Z. Liu, C. L. P. Chen, C. L. Zhang, K. R. Chen, Finite-time consensus control for multi-agent systems with full-state constraints and actuator failures, *Neural Networks*, **157** (2023), 350–363. https://doi.org/10.1016/j.neunet.2022.10.028

32. D. J. Yao, C. X. Dou, N. Zhao, T. J. Zhang, Practical fixed-time adaptive consensus control for a class of multi-agent systems with full state constraints and input delay, *Neurocomputing*, **446** (2021), 156–164. https://doi.org/10.1016/j.neucom.2021.03.032

33. J. H. Wang, Q. J. Gong, K. F. Huang, Z. Liu, C. L. P. Chen, J. Liu, Event-triggered prescribed settling time consensus compensation control for a class of uncertain nonlinear systems with actuator failures, *IEEE Trans. Neural Networks Learn. Syst.*, **34** (2023), 5590–5600. https://doi.org/10.1109/TNNLS.2021.3129816

34. Y. Zhao, H. Yu, X. H. Xia, Event-triggered adaptive control of multi-agent systems with saturated input and partial state constraints, *J. Franklin Inst.*, **359** (2022), 3333–3365. https://doi.org/10.1016/j.jfranklin.2022.04.004

35. W. Wang, D. Wang, Z. H. Peng, T. S. Li, Prescribed performance consensus of uncertain nonlinear strict-feedback systems with unknown control directions, *IEEE Trans. Syst., Man, Cybern.: Syst.*, **46** (2016), 1279–1286. https://doi.org/10.1109/TSMC.2015.2486751

AIMS Press